



STRAIN READING CORRECTION FOR APPARENT STRAIN AND THERMAL EXPANSION COEFFICIENT OF MASONRY AND BRICK

A.V. Gayevoy¹ and S.L. Lissel²

¹M.Sc. Candidate, Dept of Civil Engineering, University of Calgary, 2500 University Dr. NW, Calgary, AB, T2N 1N4, agayevoy@ucalgary.ca

²Assistant Professor, Dept of Civil Engineering, University of Calgary, slissel@ucalgary.ca

ABSTRACT

Two CFRP prestressed diaphragm masonry walls built on the University of Calgary campus are the subject of an ongoing monitoring program. Two short-term monitoring sessions were held to investigate the influence of the solar radiation on the masonry strains. During data processing some unexpected observations in the readings were made. Upon further investigation the influence of temperature and the resulting apparent strain was recognized. The subsequent study showed the necessity to determine the Coefficients of Thermal Expansion (CTE) of brick and masonry used for the wall's construction. This paper discusses the motives and background of the CTE tests, describes the test procedure and reports the results. Also, the readings from the two short-term monitoring sessions corrected for the apparent strain influence are presented and discussed.

KEYWORDS: electric resistance strain gauge, apparent strain, coefficient of thermal expansion, monitoring

INTRODUCTION

In the summer of 2002 two masonry diaphragm retaining walls prestressed with CFRP tendons were built on the University of Calgary campus [1]. The purpose of this construction was to monitor the behaviour of such walls under real environmental and structural loads. After the walls' design was complete and the footing had been constructed, changes in landscaping took place. It was not possible to modify the design at that point, therefore monitoring the behaviour and prestress losses due to temperature variation became most interesting as the structural loads turned out to be much less than the loads used for designing the walls. The characteristics being monitored are: strain in tendons, strain in the masonry and bricks, as well as temperature at the locations of the strain gauges and in the cavity. Simple but precise instruments were used to take initial readings and for subsequent periodic monitoring. At a location (top of south face) subject to significant amounts of direct sunlight, the temperature effects were quite significant. After observing unexpected trends in the strain gauge readings at this location, it was deemed necessary to conduct short-term continuous monitoring sessions with a relatively high sampling rate (1 reading/5 minutes) [2]. The main reason for conducting these programs was to evaluate closely the influence of solar radiation on the brick/masonry strain behaviour. The data acquisition system available would not operate in cold temperatures so in summer 2003 two monitoring sessions were executed on one of the walls. The results of these sessions made

obvious the difference between strain readings taken from the shadowed parts of the wall and the location exposed to direct sun light. Upon processing of the data, there appeared to be some problems with the strain readings [3]. After a more in depth investigation it was determined that the collected data included temperature induced apparent strain bringing systematic error to the strain readings.

TEMPERATURE INDUCED APPARENT STRAIN

Temperature induced apparent strain is a strain reading that would be registered by a strain indicator connected to a strain gauge (SG) bonded to a specimen while both are subjected to varying temperature. It results from the difference in Coefficients of Thermal Expansion (CTEs) of the specimen and strain gauge materials. Also, the electrical resistivity of the strain gauge itself deviates when temperature varies. The temperature induced apparent strain $\epsilon_{APP(S/G)}$ can be expressed as the sum of these two effects, as shown in Equation 1 [4].

$$\epsilon_{APP(S/G)} = \left[\frac{\beta_G}{F} + (\alpha_S - \alpha_G) \right] \Delta T \quad \text{Equation 1}$$

In this equation β_G is the thermal coefficient of resistance of the grid conductor (strain gauge), F is the gauge factor, α_S and α_G are the CTE of the substrate (specimen) and grid (gauge) materials respectively, and ΔT is the temperature change measured with respect to the arbitrary initial reference temperature (T_R in Equation 2). Apparent strain depends on the properties of both the grid/gauge (subscript G) and substrate/specimen (subscript S) materials. The terms in the brackets are dependant on temperature themselves, thus the apparent strain is not a linear function.

There is a technique to compensate for apparent strain which involves attaching a dummy gauge to an unloaded specimen and connecting the gauge in a $\frac{1}{2}$ bridge circuit with the active gauge. Of course, both specimens have to be placed in the same environment and the dummy and active gauges should be selected from the same shipment, and ideally from the same package. In these walls the $\frac{1}{2}$ bridge configuration has been used for the tendon strain monitoring however it was not possible to place an unloaded specimen in every location of a masonry strain gauge. When the dummy gauge in the $\frac{1}{2}$ bridge circuit is replaced instead with a temperature stable invariable resistor, a $\frac{1}{4}$ bridge circuit is used and then apparent strain should be compensated for during data analysis.

COMPENSATION FOR APPARENT STRAIN

Correcting data for apparent strain involves simple subtraction of the known apparent strain from the raw in-situ strain reading. For more precise compensation, the result of the subtraction can be corrected for gauge factor variation as it deviates slightly with temperature as well. The difficulty is to calculate the apparent strain since very specific information is required for this procedure.

Each package of strain gauges contains an engineering data sheet providing technical information specific to each particular shipment. Among other information, it contains a graph plotted from the apparent strain laboratory test conducted on gauges selected from the shipment. It also specifies the conditions of the laboratory test as well as other valuable data. Fragments of such a sheet are displayed in Figure 1.

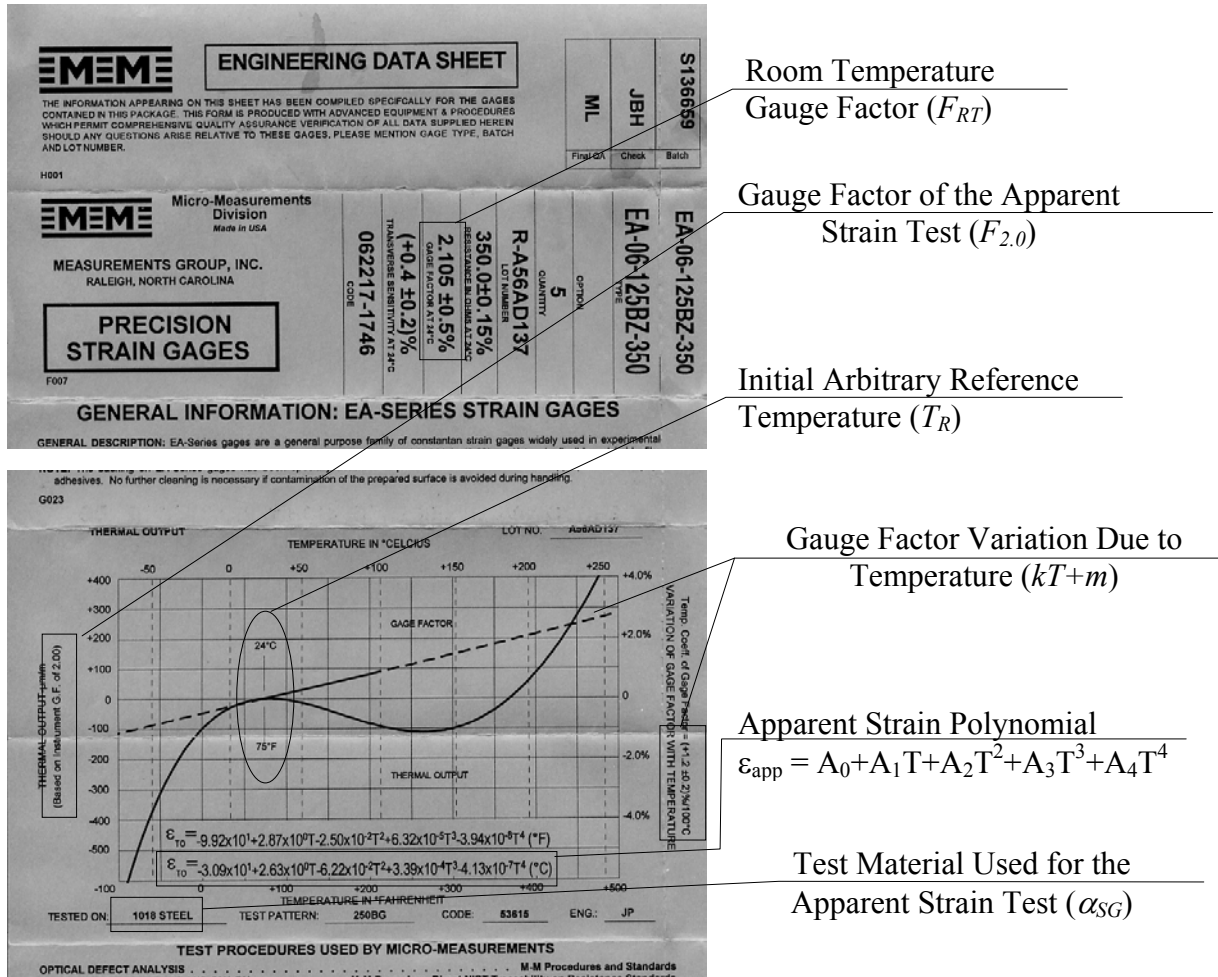


Figure 1 – Fragments of a Strain Gauge Engineering Data Sheet [5]

All the data specified in Figure 1 are necessary for apparent strain correction especially the apparent strain polynomial (Equation 2). The final formula for correction is somewhat complex as it has to incorporate all of this information as shown in Equation 2. It is important to note that this equation contains the CTE of the in-situ substrate/specimen material, α_{ST} . The apparent strain polynomial presented on the data sheet (Figure 1) is precise for the particular combination of strain gauge and substrate material used in the laboratory test with known CTE, α_{SG} . To be able to use the polynomial for the in-situ substrate material the difference between the CTEs should be applied in the correction. Thus, it is absolutely necessary to determine the CTE of masonry and brick to achieve precise data correction for apparent strain.

$$\epsilon_{app} = A_0 + A_1T + A_2T^2 + A_3T^3 + A_4T^4 \quad \text{Equation 2}$$

$$\epsilon' = \frac{\epsilon_R - \left[A_0 + A_1T + A_2T^2 + A_3T^3 + A_4T^4 \right] \frac{F_{2.0}}{F_{RT}}}{\left(1 + \frac{kT + m}{100} \right)} - (\alpha_{ST} - \alpha_{SG})(T - T_R) \quad \text{Equation 3}$$

DETERMINING CTE WITH ELECTRICAL RESISTANCE STRAIN GAUGES

It was necessary to determine the “instantaneous” rather than “linear” CTE of brick and masonry because of the wide temperature range in the in-situ monitoring program. An existing procedure for the measurement of CTE using strain gauges was used [6]. The concept is that the difference in CTEs of two materials (α_S and α_R) will be equal to the difference in apparent strain measured on these two materials ($\varepsilon_{app(S/G)}$ and $\varepsilon_{app(R/G)}$) divided by the difference in temperature (ΔT) since, if the same gauges are used on the two materials, Equation 1 can be rearranged to give Equation 4. In the equation, subscripts “S” refer to the substrate/specimen, subscripts “R” to the reference, and subscripts “G” to the grid/gauge materials.

$$\alpha_S - \alpha_R = \frac{(\varepsilon_{APP(S/G)} - \varepsilon_{APP(R/G)})}{\Delta T} \quad \text{Equation 4}$$

It was also decided that it would be good practice to fulfill the ASTM requirements if possible [7]. ULETM (Ultra Low Expansion) Titanium Silicate Glass was used as the reference material in the CTE test [8]. This material demonstrates high strain stability under temperature variation, much like an INVAR bar. Its CTE measures in tenths of PPM/°C even at a temperature as low as -75°C (Figure 2). The requirement for a “temperature stable” ¼ bridge completion resistor is not to exceed 1.0 PPM/°C temperature dependence [4]. Thus, it is reasonable to neglect the CTE of the reference material, α_R , simplifying Equation 4.

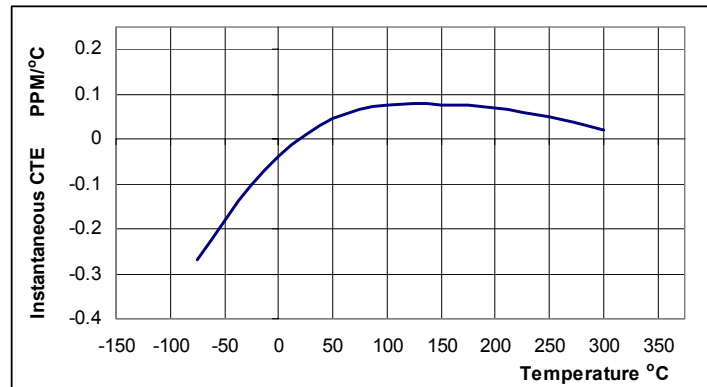


Figure 2 – CTE of Reference Material Used in the Chamber Test [8]

The masonry and reference material specimens with the attached strain gauges were placed in a controlled temperature chamber. The number of the strain gauges as shown in Figure 3 refers to the length of strain gauge (30, 50, and 100 mm). The letters “R” and “S” in the subscript refer to gauges on the reference and the substrate/masonry specimens, respectively. The number 2 in the subscript refers to gauges that were placed on the opposite side of the masonry specimen. A pan of water was placed in the chamber to provide some humidity since the natural in-chamber relative humidity was only about 4%. The temperature was cycled between -40°C and +50°C at a relatively slow rate of 0.1°C/min.

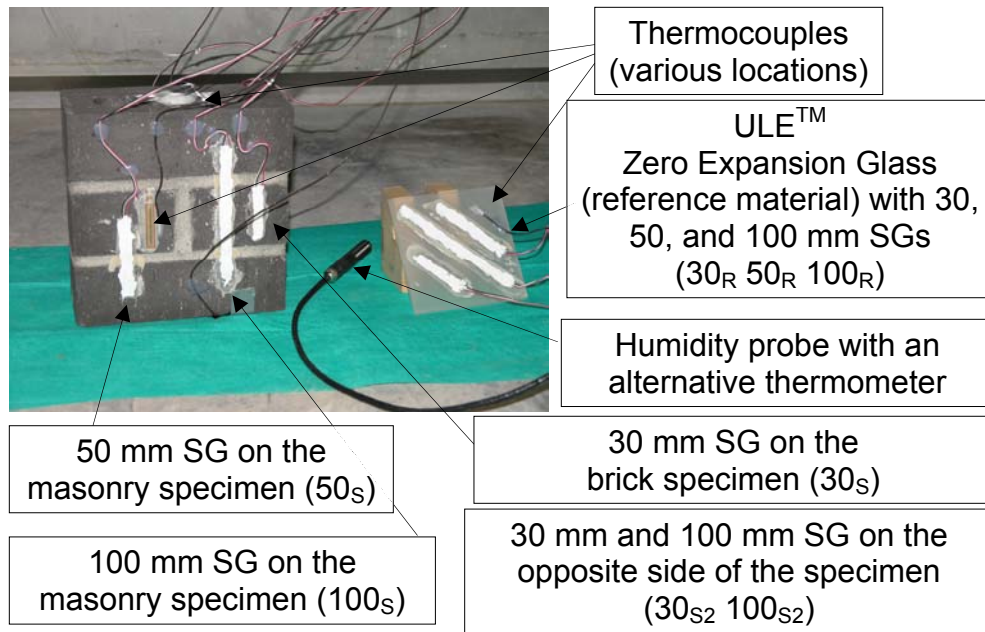


Figure 3 – CTE Test Specimens

During the analysis of the data from this test it was observed that two of the gauges, 100_{S2} and 30_{S2} , demonstrated somewhat abnormal trends similar to those that had been observed in SGs attached to the top of the south face of the wall [3]. The fact that this abnormality appeared in a controlled test was of particular interest. Further data analysis also showed that there was a fixed time-point at which one of the two gauges radically changed its behaviour. A partial debonding of the gauge was suspected. Subsequent visual inspection of the specimen proved this to be the case for both gauges.

The test data were analyzed and apparent strain polynomials similar to those provided on engineering data sheets (Figure 1) were derived. It was important to reduce them to the same initial arbitrary reference temperature as on the engineering data sheet (+24°C). The results of these calculations are summarized in Table 1. The equation of the material's instantaneous CTE is determined by taking the first derivative of the subtraction of the two apparent strain equations:

$$\text{CTE} = [\varepsilon_{\text{app (G/S)}} - \varepsilon_{\text{app (G/R)}}]' = B_0 + B_1 T + B_2 T^2 + B_3 T^3 \quad \text{Equation 5}$$

These calculations are summarized in Table 2. The charts for the CTEs have been plotted in Figure 4. It can be observed from the charts that CTE of masonry determined by the 100 mm gauges and alternatively by the 50 mm strain gauges are close, especially over the temperature range of -20 to +30 °C. It should be noted that the 50 mm gauge crosses only one mortar joint while the 100 mm gauge crosses 2 joints and a whole brick. In fact the 50 mm gauge produces a curve that is nearly horizontal but still has greater CTE than brick within the practical temperature range (-30 to +35 °C). The CTE of masonry (both 50 and 100 mm gauge) at moderate temperatures (10-25°C) is almost constant and within the reported ranges of 3.1 to 12.4 PPM/°C [9]. The CTE of brick does not fit the reported range of 4.5 to 7.2 PPM/°C [9].

However, the CTE of the brick is lower than that for the masonry which is logical. These observations allow us to conclude that the test was successful and the CTE test data are reliable for further processing.

Table 1 – Apparent Strain Equation Coefficients

$\epsilon_{app} = A_0 + A_1T + A_2T^2 + A_3T^3 + A_4T^4$ (Equation 2)						
	30 _S	30 _R	50 _S	50 _R	100 _S	100 _R
A ₄ =	4.00E-06	-6.00E-07	2.00E-06	1.00E-07	6.00E-06	4.00E-08
A ₃ =	5.00E-04	3.00E-04	4.00E-04	4.00E-04	3.00E-04	3.00E-04
A ₂ =	-0.047	-0.054	-0.063	-0.066	-0.062	-0.062
A ₁ =	-6.000	-8.928	-3.608	-8.613	-0.703	-6.559
A ₀ =	162.842	241.310	116.848	239.163	46.669	188.977
R ² =	0.9841	0.9998	0.969	0.9996	0.4683	0.9994

Table 2 – Calculations for the Materials' CTEs

$[\epsilon_{app} (G/S) - \epsilon_{app} (G/R)]$				CTE = B ₀ + B ₁ T + B ₂ T ² + B ₃ T ³			
	Brick 30 _S – 30 _R	Masonry 50 _S – 50 _R	Masonry 100 _S – 100 _R		Brick	Masonry (50)	Masonry (100)
A ₄	4.60E-06	-1.90E-06	5.96E-06				
A ₃	2.00E-04	0.00E+00	0.00E+00	B ₃	0.000018	-7.60E-06	2.38E-05
A ₂	0.007	0.003	0.000	B ₂	0.001	0.000	0.000
A ₁	2.928	5.005	5.856	B ₁	0.014	0.005	-0.001
A ₀	-79.340	-132.136	-142.308	B ₀	2.928	5.005	5.856

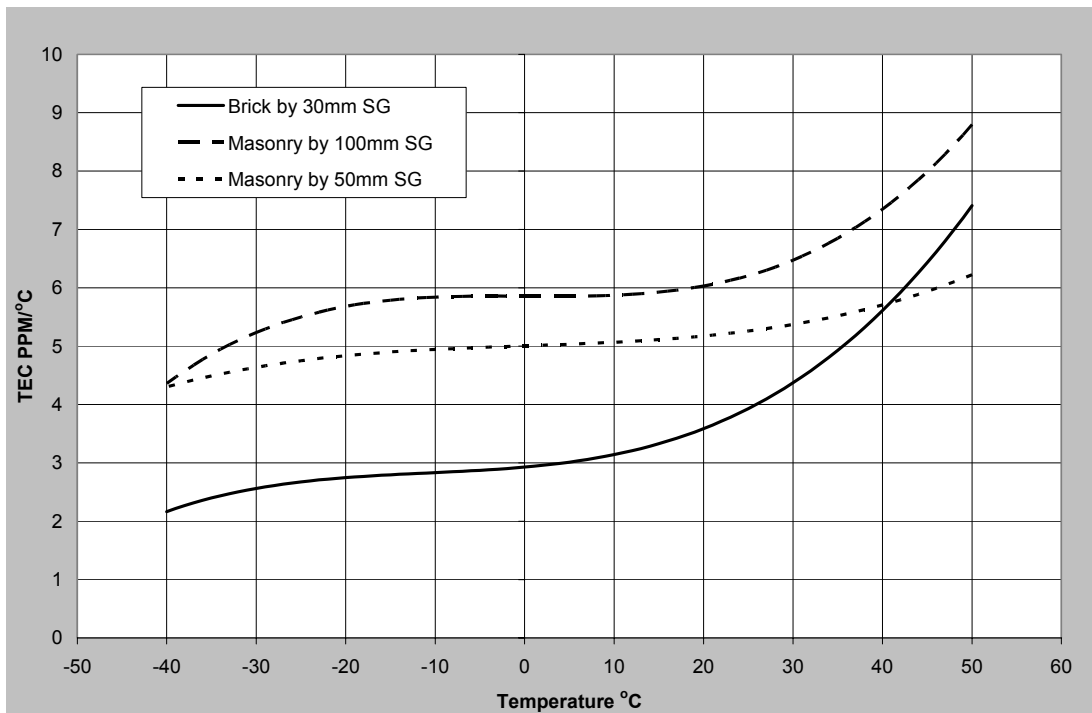


Figure 4 – Material CTEs Determined By Test

RESULTS AND DISCUSSION

As mentioned before, the CTEs were determined to be used in Equation 2. However, a simplification can be made when apparent strain in the CTE test was measured using strain gauges from the same package that were used for the in-situ monitoring. In this case, the in-chamber measured apparent strain should be subtracted directly from the raw in-situ collected strain and the resultant may be used for further data analysis. Therefore the corresponding polynomials presented in Table 1 can be used for this convenient correction.

The first example of correction for apparent strain to be considered here is the 30 mm strain gauge located at the bottom of the wall in the centre of the north face (Figure 5). The apparent strain for the substrate and reference materials was calculated from the corresponding polynomial for the temperature at the point (thin solid line) and this was subtracted from the raw readings (dashed line). This gives two different results: 1) The dotted line is for the strain readings corrected for apparent strain recorded from the SG on the substrate material. Thus the temperature induced apparent strain is accounted for, and the corrected data represent strain variation due to change in the mechanical load on the walls. Since the lateral loads are constant the only change in loading is due to changes in prestressing force. As the temperature decreases, there is a loss of force in the CFRP prestressing tendons. This loss of prestress corresponds to a decrease in compressive strain (positive strain change). Thus, the dotted line demonstrates what it is expected. 2) The thick solid line is for the strain readings corrected for apparent strain recorded from the SG on the reference material and shows the total strain deviation (due to changes in temperature and mechanical load) during the monitoring session. The total strain variation does not follow the diurnal cycle expressly because elastic stress redistribution due to loss in prestress partially counteracts the contraction due to temperature decrease, thereby flattening the curve.

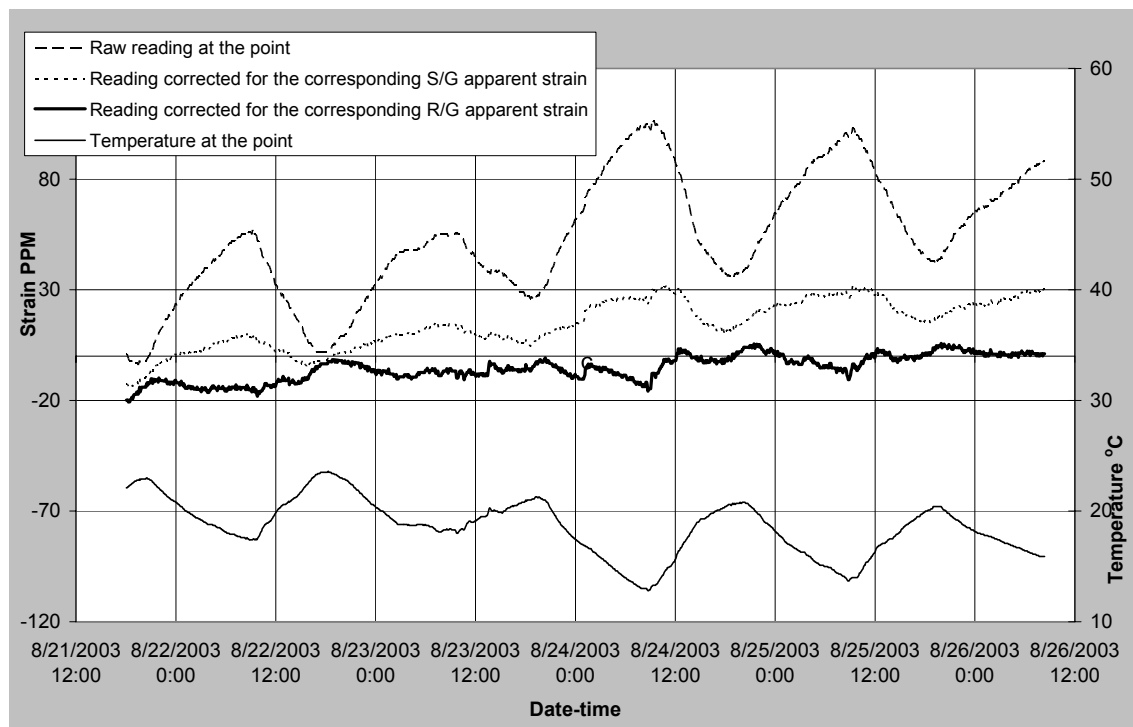


Figure 5 – 30 mm SG North Face Centre Lower Raw and Corrected Strain Readings

Another 30 mm strain gauge located at the bottom of the south face at the east end, was corrected by the same method (Figure 6). However, here the corrected readings do not follow the same patterns as those on the previous figure. The reason for this difference could be that the temperature recorded at the south face (insulated by retained soil) is almost constant and the maximum temperature variation is only half that recorded on the north face (4°C vs. 8°C). The effect from apparent strain correction is not as evident at such a narrow temperature range.

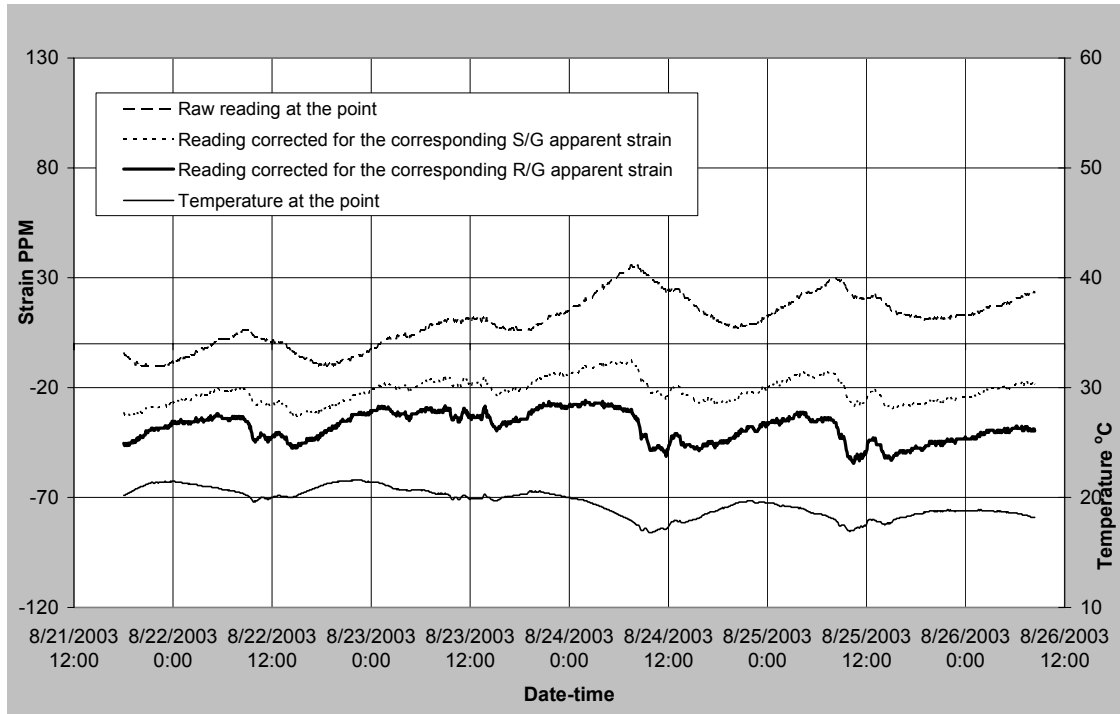


Figure 6 – 30 mm SG South Face East End Lower Raw and Corrected Strain Readings

Finally, a 100 mm SG attached to an unloaded control prism installed inside of the wall is considered (Figure 7). The first observation to be made from this chart is that the initial raw reading and strain corrected for S/G apparent strain look identical. This is partly because of a narrow temperature range like in the previous case. The previous two cases were for strain in brick only, while the 100 mm gauges cross over two mortar joints as well. Still, one would expect the readings corrected for S/G apparent strain to form a flat line since no load was applied to the control prism. This inconsistency can be explained in part by the nature of the masonry CTE which is dependent on the CTE of its two components: brick and mortar. The CTE of paste, which is a component of mortar, has been shown to be dependant on relative humidity in a complicated manner [10]. Figure 8 shows the characteristic dependence of mortar CTE on relative humidity changes with aging. No reports on the dependence of the CTE of brick on relative humidity were found.

One would not expect the dependence on relative humidity to be so significant for masonry where the mortar accounts for a maximum of 20% of the material, however, there would still be some effect.

The specimens used for the CTE test were about 6 months old and had been aged in the lab environment which has a fairly constant relative humidity (RH) of about 25%. During the CTE test, the relative humidity in the chamber was also kept constant, at about 28% RH. So it is fair to say that the CTE of the specimens used for the CTE test would not have been affected by the phenomenon shown in Figure 8. The walls were constructed in the summer when the RH can vary drastically with the weather and the RH in the wall cavities has continued to be variable, usually 20 to 30% higher than the ambient relative humidity. In addition the age of the walls was nearly 2 years when the sessions were held. This longer period of aging at a more variable RH could have an influence on the CTE of the masonry in the walls and thus the apparent strain corrections.

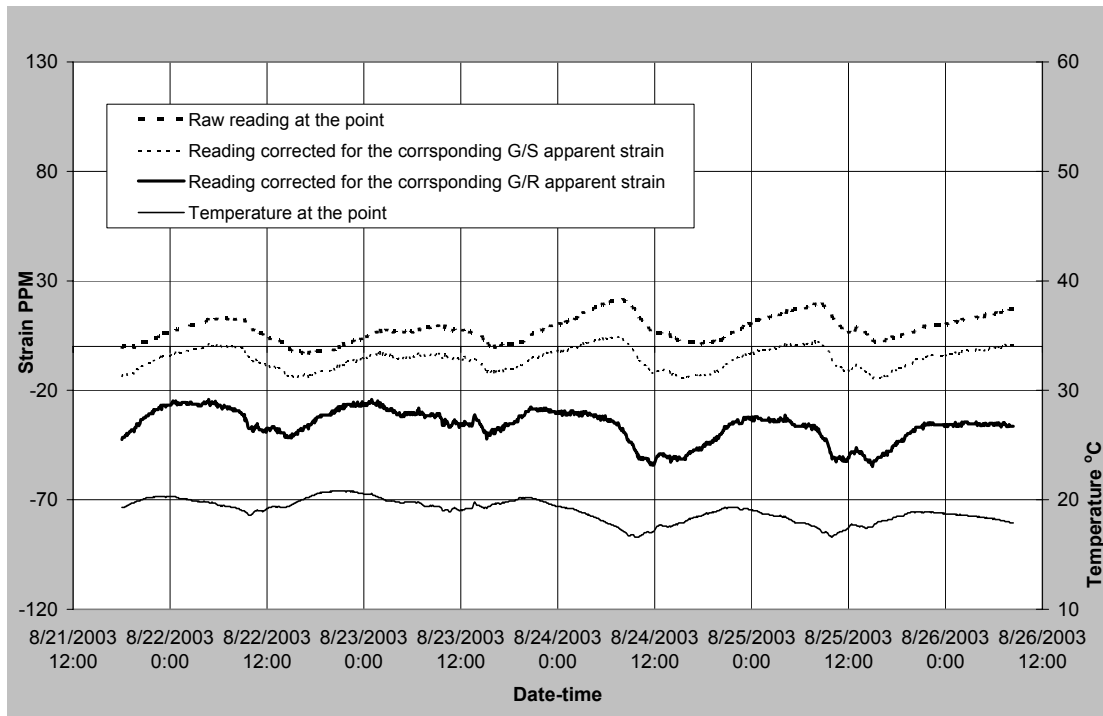


Figure 7 – 100 mm SG Control Prism Raw and Corrected Strain Readings

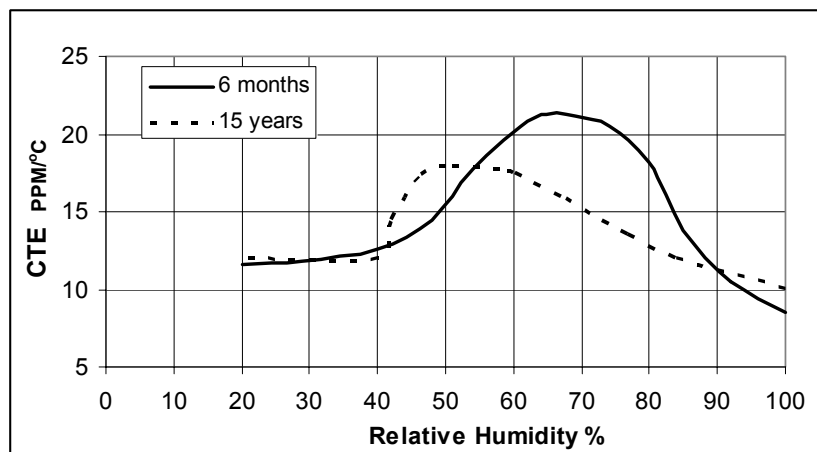


Figure 8 – Dependence of CTE of Mortar on RH [10]

SUMMARY

In order to correct the strain data collected during a four-day continuous monitoring session, the instantaneous CTEs of brick and masonry were experimentally determined. The test results were within normal ranges reported in the literature and the CTE of brick was found to be less than that of masonry as expected since the CTE of mortar is generally greater than that of masonry. The apparent strain recorded during the CTE chamber test was applied for apparent strain compensation of the in-situ strain readings. This was possible because the strain gauges used for the CTE test were taken from the same shipment as those used for the in-situ monitoring. It was observed that apparent strain compensation has a noticeable effect when considerable temperature variations take place.

ACKNOWLEDGEMENTS

The authors would like to acknowledge Corning Incorporated for the ULE™ (Ultra Low Expansion) Titanium Silicate Glass generously donated to the U of C Civil Engineering Department Laboratory. Many thanks to Don McCullough and Dan Tilleman, laboratory technical staff, for their aid in the test work. Also, advice from Dr. Nigel Shrive and access to his library is gratefully acknowledged.

REFERENCES

1. Lissel S.L., Gilliland J., and Shrive N.G. Design of Two Demonstration CFRP Post-Tensioned Masonry Diaphragm Retaining Walls. Proceedings of the British Masonry Society, No 9, British Masonry Society. London, UK. Nov. 2002.
2. Gayevoy, A.V., and Lissel, S.L. Structural Health Monitoring of FRP Prestressed Masonry Walls. 6th Cansmart Meeting - International Workshop on Smart Materials and Structures. Montreal, Quebec Canada. 2003.
3. Gayevoy A.V. and Lissel S.L. Monitoring of FRP Prestressed Masonry Walls. 13th International Brick/Block Masonry Conference. Amsterdam, Netherlands. 2004.
4. Measurements Group Inc. Temperature-Induced Apparent Strain and Gage Factor Variation in Strain Gauges. Tech Note TN-504. Raleigh, North Carolina, US. 1976.
5. Measurements Group Inc. Precision Strain Gauges. Engineering Data Sheet. Raleigh, North Carolina, US.
6. Measurements Group Inc. Measurement of Thermal Expansion Coefficient Using Strain Gauges. Tech Note TN-513. Raleigh, North Carolina, US. 1986.
7. ASTM E251-92. Metals Test Methods and Analytical Procedures. Annual Book of ASTM Standard, v. 03.01. 2004
8. Corning Inc. Zero Expansion Glass ULE™. Technical Sheet in Catalogue. Canton, NY, US. 1998.
9. Drysdale R.G. Masonry Structures Behavior and Design. Second Edition. The Masonry Society. Boulder, Colorado, US. 1999
10. Neville A.M. Properties of Concrete. Longman Scientific & Technical. Harlow, UK. 1996